MAPPING TRENDS OF CARBON DIOXIDE AND METHANE DURING MOVEMENT CONTROL ORDER IN INDUSTRIAL AREAS IN PENINSULAR MALAYSIA USING GOSAT, GOSAT-2, OCO-2, OCO-3, AND TROPOMI SATELLITES DATA

Hui Lin Ng[1], Mazlan Hashim[1, 2]

[1]Department of Geoinformation, Faculty of Built Environment and Surveying, Universiti Teknologi Malaysia, 81310 Johor Bahru, Johor Darul Ta'zim, Malaysia.
[2]Geoscience and Digital Earth Centre (INSTeG), Faculty of Built Environment and Surveying, Universiti Teknologi Malaysia, 81310 Johor Bahru, Johor Darul Ta'zim, Malaysia.

Commission IV, WG VII

KEY WORDS: Carbon dioxide, methane, industrial area, GOSAT, GOSAT-2, OCO-2, OCO-3, TROPOMI.

ABSTRACT:

The Malaysian government implemented the Movement Control Order (MCO) from March 18 to May 13, 2020, in an effort to curb the coronavirus disease outbreak that had spread throughout the nation. Utilizing data from GOSAT, GOSAT-2, OCO-2, OCO-3, and TROPOMI, the total column-averaged dry-air mole fraction of carbon dioxide and methane (referred as XCO_2 and XCH_4) is employed to examine the patterns of both gases throughout the MCO as well as from the same period the prior and following year. The Inverse Distance Weighting (IDW) interpolation method is utilized in mapping the XCO_2 and XCH_4 for the industrial areas in Peninsular Malaysia. The results revealed that even MCO is implemented, the XCO_2 and XCH_4 in the industrial areas are increasing year by year. By using satellites data, the XCO_2 and XCH_4 from large areas can be monitored continuously.

1. INTRODUCTION

1.1 Background

More than 500 million people worldwide have contracted coronavirus disease (COVID-19), which has also resulted in more than 6 million fatalities. The World Health Organization (WHO) had designated the COVID-19, an infectious illness brought on by the SARS-CoV-2 virus (WHO, 2022), to be a pandemic on March 11, 2020 (Ducharme, 2020), after it was first detected in Wuhan, China, in November 2019 (Ma, 2020). Over a hundred nations had either a partial lockdown or a full lockdown in place by the end of March 2020 Following the confirmation of the first cases of COVID-19 on January 25, 2020 (Loheswar, 2020), a nationwide Movement Control Order (MCO) was enforced in Malaysia from March 18 to May 3, 2020 (Phase 1: 18 to 31 March; Phase 2: 1 to 14 April; Phase 3: 15 to 28 April; Phase 4: 29 April to 3 May). Conditional MCO (CMCO) and Recovery MCO (RMCO) followed after the MCO. According to the COVID-19 infection status of each state and territory, the second MCO (MCO 2.0) was put into effect from January 13 through May 31, 2021. Following the surge in COVID-19 cases across the nation, a Full MCO (FMCO) was imposed from June 1 to June 28, 2021. Depending on the state and territorial conditions, a National Recovery Plan (NRP) was declared and began on June 15, 2021. It consists of four phases and involves the phase transitions of the MCO in stages.

The air quality had improved over the first four weeks of the MCO (18 March to 14 April) as evidenced by data observed from 65 continuous air quality monitoring (CAQM) stations in Malaysia, where the Air Pollution Index (API) readings fell by 14% to report a "clean index". Analyses done in Klang Valley had shown that the measurements of particulate matter with aerodynamic diameter below or equal to 2.5 µm ($PM_{2.5}$), carbon monoxide (CO), nitrogen dioxide (NO_2), and sulfur dioxide (SO_2) had decreased by 29%, 49%, 70%, and 27%, respectively, compared to prior MCO period. Pollutants in other major cities and towns also decreased by 26%, 31%, 61%, and 40% for $PM_{2.5}$, CO, NO_2, and SO_2, respectively (Babulal, 2020). Among the 65 stations, besides one station that is categorized as the background station, 34, 12, and 11 stations are located at sub-urban, rural, and urban area, respectively, while only 7 stations are situated at industrial area (Ash'aari et al., 2020). With the limited number of stations, data from the CAQM stations are too sparse to cover the whole nation. Due to the location of the stations that are away from the emission sources, high spatial resolutions data are unable to be obtained although they provide a good overview of the air quality (Nadzir et al., 2020). Hence, satellite data can be used for air quality monitoring as these datasets have a larger spatial coverage compared to CAQM stations. Therefore, the primary goal of this paper is to map trends of CO_2 and CH_4 during MCO period in industrial areas in Peninsular Malaysia using Greenhouse gases Observing SATellite / Thermal And Near infrared Sensor for carbon Observation - Fourier Transform Spectrometer (GOSAT/TANSO-FTS, hereafter referred to as GOSAT), GOSAT-2/TANSO-FTS-2 (hereafter referred to as GOSAT-2), Orbiting Carbon Observatory -2 and -3 (OCO-2 and OCO-3), and Sentinel-5 Precursor / TROPOspheric Monitoring Instrument (S5P/TROPOMI, hereafter referred to as TROPOMI) satellite data.

During MCO and FMCO, movements were restricted and operations of premises were ceased except for essential services. Non-essential industries were shut down during these periods. In this study, the trend of carbon dioxide (CO_2) and methane (CH_4) of industrial areas in Peninsular Malaysia were analysed as data of CO_2 and CH_4, the most and second most important greenhouse gases (GHGs) were not monitored by the CAQM stations. GOSAT, GOSAT-2, OCO-2, OCO-3, and TROPOMI were employed to monitor the CO_2 and CH_4 in industrial areas during the MCO. The CO_2 and CH_4 throughout this duration of the study were evaluated to the same time from

the years prior and following the MCO, depending on the data availability.

1.2 Study Area

Currently, there are over 600 industrial estates in Malaysia (MIDA, 2020). Air pollutants were emitted from a total of 13,776 industrial sources as at December 2020, where the highest sources were in Selangor (21%), Johor (18%) and Perak (11%) (DOE, 2021). Figure 1 illustrates the study area, which are the industrial areas in Peninsular Malaysia. The East Malaysia is not included in this study.

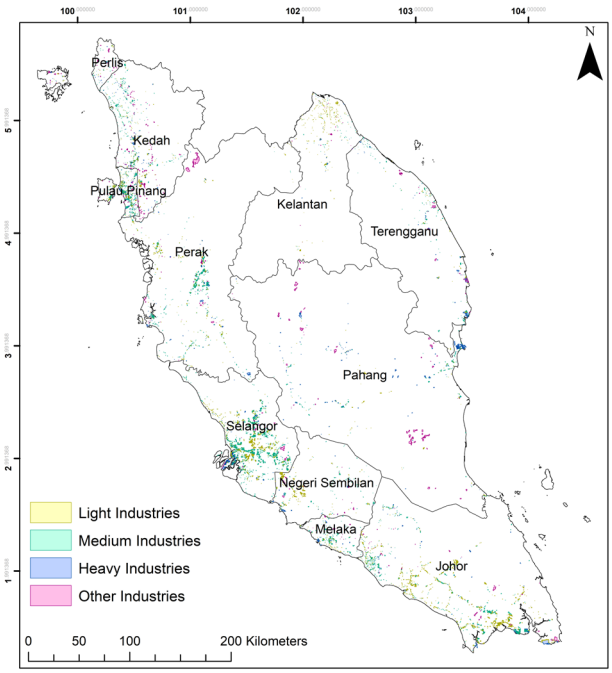

Figure 1. Industrial areas in Peninsular Malaysia.

2. METHODOLOGY

2.1 Data

Level 2 data of total column-average dry-air mole fraction of CO_2 and CH_4 (denoted as XCO_2 and XCH_4, respectively) from GOSAT, GOSAT-2, OCO-2, OCO-3, and TROPOMI were used in this study. XCO_2 data were obtained from GOSAT, GOSAT-2, OCO-2, and OCO-3 while XCH_4 were provided by GOSAT, GOSAT-2, and TROPOMI. Data for the full period of MCO (18th March to 3rd May) of year 2019, 2020, and 2021 for all satellites were employed except for OCO-3 XCO_2 data, where only data for the year 2020 and 2021 were used due to the data availability.

GOSAT, also known as Ibuki, is a joint project of the Japan Aerospace Exploration Agency (JAXA), the National Institute for Environmental Studies (NIES), and the Japanese Ministry of Environment (MOE), which was launched on January 23, 2009 (Chevallier et al., 2009). It is the first satellite designed specifically for measuring CO_2 and CH_4 concentrations near the Earth's surface with good sensitivity (Shim et al., 2019). The satellite has a sun-synchronous descending polar orbit which cross the Equator at 13:00 local time (LT) (Chevallier et al., 2009). Due to its 666 km orbit, it can cover the entire planet in around 3 days by completing one orbit approximately every 100 minutes (Shim et al., 2019). GOSAT footprints are 10.5 km at nadir and the soundings are separated by ~ 158 km across track and ~ 152 km along track when five-point across track mode was used prior to 1st August 2010. The footprints are spaced by ~ 263 km across track and ~ 283 km along track after it was switched to three-point across track mode (Heymann et al., 2015). TANSO-FTS, one of the two instruments onboard GOSAT, provides CO_2 and CH_4 column measurements with near-surface sensitivity using three narrow shortwave infrared (SWIR) bands at 0.76, 1.6, and 2.0 µm and with mid-tropospheric sensitivity using the fourth thermal infrared (TIR) band spanning between 5.5-14.3 µm (Parker et al., 2016). The bias corrected XCO_2 (v02.97 and v02.98) and XCH_4 (v02.95 and v02.96) data used are downloaded from the GOSAT Data Archive Service (GDAS; https://data2.gosat.nies.go.jp/index_en.html).

The GOSAT-2, the successor of GOSAT, was launched on October 29, 2018, into a 613 km sun-synchronous orbit with a revisit time of 6 days and an Equator crossing time of 13:00 LT. The TANSO-FTS-2 instrument was improved over the TANSO-FTS onboard GOSAT. It can cover a broad spectral range in three narrow SWIR bands of 0.76, 1.6, and 2 µm and a wide TIR band in 5.5-14.3 µm (Suto et al., 2021). The XCO_2 and XCH_4 data used were downloaded from the GOSAT-2 Product Archive (https://prdct.gosat-2.nies.go.jp/index.html.en).

The National Aeronautics and Space Administration (NASA)'s OCO-2 mission was launched on July 2, 2014 (Heymann et al., 2017). This sun-synchronous polar orbiting satellite is the first satellite flying in the 705 km Earth Observing Systems (EOS) Afternoon Constellation (A-Train), and it crosses the Equator at 13:36 LT (Hakkarainen et al., 2016). The OCO-2 instrument incorporate three grating spectrometers acquiring high-resolution spectra of reflected sunlight in the 0.765 µm oxygen (O_2) A-band, and in the 1.61 and 2.06 µm weak and strong CO_2 bands (Crisp et al., 2017). With a repeat cycle of 16 days, and a narrow swath of ~ 10.3 km (Ye et al., 2020), each of the eight sounding has a spatial resolution of less than 1.29 km × 2.25 km and horizontal offsets of about 150 km can be observed between adjacent revisiting orbits (Crowell et al., 2019). This study utilizes the version 10r XCO_2 data downloaded from Goddard Earth Sciences Data and Information Services Center (GES DISC; https://disc.gsfc.nasa.gov/datasets/OCO2_L2_Lite_FP_10r/summary?keywords=oco-2).

The NASA's OCO-3 payload was attached to the Japanese Experiment Module – Exposed Facility (JEM-EF) aboard the International Space Station (ISS) (Wu et al., 2020) after a successful launch on May 4, 2019 (Srivastava et al., 2020). Its core spectrometer was the flight spare for OCO-2 (Eldering et al., 2017). Instead of overpassing at the same local time every day for a particular latitude, the ISS passes over 20 minutes earlier each day, gradually sampling the entire day from dawn to dusk. With both daylight ascending and descending nodes, the OCO-3 data cover a period of about 6 hours from local noon. The estimated repetition cycle for the ISS orbit is every 3 days, while the illumination repeat cycle is 63 days. Similar to the OCO-2 instrument, the OCO-3 spectrometer consists of three channels at 0.765 µm for the O_2 A-band, and two CO_2 bands at 1.61 µm and 2.06 µm for the weak and strong CO_2 bands, respectively (Taylor et al., 2020). The version 10.4r XCO_2 data used are downloaded from GES DISC (https://disc.gsfc.nasa.gov/datasets/OCO3_L2_Lite_FP_10.4r/summary?keywords=oco-3).

TROPOMI, funded jointly by the Netherlands Space Office and the European Space Agency (ESA), is the only payload onboard the ESA’s Copernicus S5P satellite, which was launched on October 13, 2017 (Kaplan and Avdan, 2020). This sun-synchronous, polar-orbiting satellite overpasses the Equator at 13:30 LT. Its 2600 km across-track swath wide allows daily worldwide coverage with 5.5 km × 7 km (after 6th August 2019, initially 7 km × 7 km) spatial resolution for CH_4 (Sha et al., 2021). CH_4 column is retrieved using the 0.757-0.774 µm O_2 absorption band and 2.305-2.385 µm CH_4 absorption band (Yang et al., 2020). The XCH_4 data utilized is of the offline data stream downloaded from Sentinel-5P Pre-Operations Data Hub (https://s5phub.copernicus.eu/dhus/#/home).

2.2 Method

Basically, the processing steps for all the data are similar. First of all, the data from GOSAT, GOSAT-2, OCO-2, OCO-3, and TROPOMI are georeferenced. TROPOMI are georeferenced according to its pixel size while the GOSAT, GOSAT-2, OCO-2, and OCO-3 data are georeferenced into 1° × 1° map. The georeferenced data of each satellite are then mosaiced into new raster images based on the date of the phases of MCO period. The Inverse Distance Weighting (IDW) interpolation is then performed to map the XCO_2 and XCH_4 in Peninsular Malaysia. The weighting coefficient and pixel size is set into 2 and 0.05° respectively for conducting the interpolation. The XCO_2 and XCH_4 in the industrial areas are then clipped from the interpolation maps based on the polygons of these areas. Finally, XCO_2 and XCH_4 maps during MCO are produced for the industrial areas in Peninsular Malaysia.

3. RESULTS AND DISCUSSION

3.1 Trends of XCO2 and XCH4 during MCO in industrial areas in Peninsular Malaysia

The maps of XCO_2 and XCH_4 produced from different satellite data during MCO are presented in Figure 2.

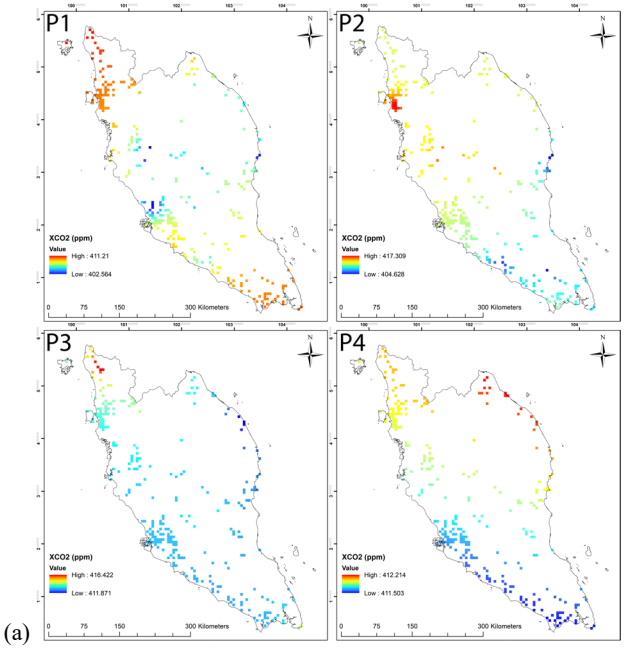

(a)

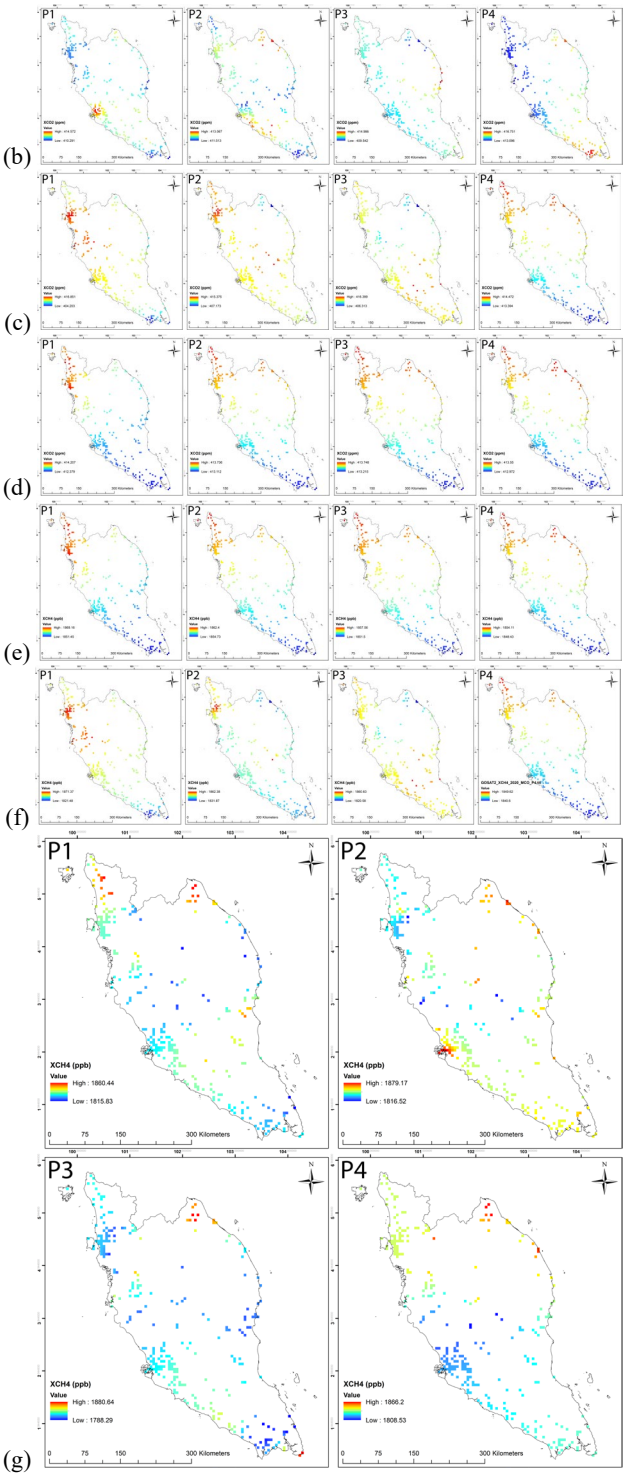

(b) (c) (d) (e) (f) (g)

Figure 2. XCO_2 and XCH_4 maps during MCO: (a) OCO-3 XCO_2, (b) OCO-2 XCO_2, (c) GOSAT-2 XCO_2, (d) GOSAT XCO_2, (e) GOSAT XCH_4, (f) GOSAT-2 XCH_4, and (g) TROPOMI XCH_4

The XCO_2 of GOSAT, GOSAT-2, OCO-2, and OCO-3 during the MCO periods for the year 2019, 2020, and 2021 are in the range of 387.911-416.255 ppm, 402.564-417.309 ppm, and 409.473-419.712 ppm, respectively. Meanwhile, for the XCH_4, the data are ranged between 1722.49-1874.82 ppb, 1788.29-1880.61 ppb, and 1768.65-1896.81 ppb, respectively, for 2019, 2020, and 2021. The average XCO_2 and XCH_4 during the periods of MCO from 2019 to 2021 are illustrated in Figure 3

and the differences between each MCO phases during these three years were tabulated in Table 1.

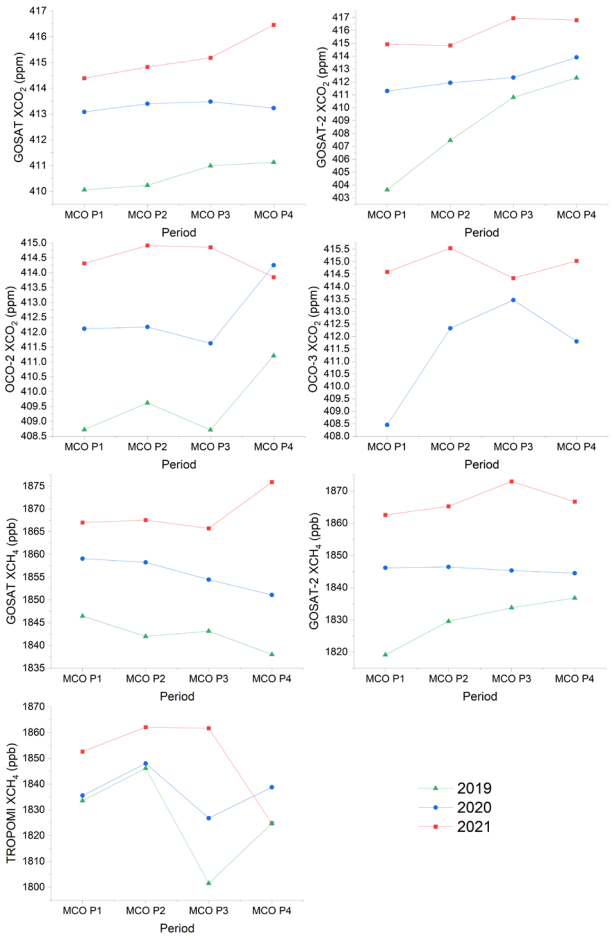

Figure 3. Average XCO_2 and XCH_4 during the period of MCO from 2019 to 2021.

Data		MCO P1		MCO P2		MCO P3		MCO P4	
		2019 to 2020 (%)	2020 to 2021 (%)	2019 to 2020 (%)	2020 to 2021 (%)	2019 to 2020 (%)	2020 to 2021 (%)	2019 to 2020 (%)	2020 to 2021 (%)
XCO_2	GOSAT	+0.74	+0.32	+0.77	+0.34	+0.61	+0.41	+0.51	+0.78
	GOSAT-2	+1.90	+0.88	+1.10	+0.70	+0.37	+1.12	+0.39	+0.70
	OCO-2	+0.83	+0.53	+0.62	+0.67	+0.71	+0.78	+0.74	-0.10
	OCO-3	-	+1.50	-	+0.78	-	+0.21	-	+0.78
XCH_4	GOSAT	+0.68	+0.43	+0.88	+0.50	+0.62	+0.61	+0.71	+1.34
	GOSAT-2	+1.49	+0.89	+0.92	+1.02	+0.63	+1.50	+0.42	+1.20
	TROPOMI	+0.11	+0.93	+0.10	+0.76	+1.40	+1.91	+0.77	-0.76

Table 1. Differences of average XCO_2 and XCH_4 during MCO periods from 2019 to 2021.

It is noted that both the average XCO_2 and XCH_4 show an increasing trend for almost all phases of MCO during 2019 to 2021 except for OCO-2 XCO_2 and TROPOMI XCH_4 for MCO Phase 4 of 2020 to 2021. The increase of XCO_2 and XCH_4 is between 0.1 to 1.91% while the decrease is approximately 0.1 to 0.76%.

The average XCO_2 and XCH_4 during MCO from March 18 to May 3, 2020 is shown in Figure 4 while the differences between each phase is as in Table 2.

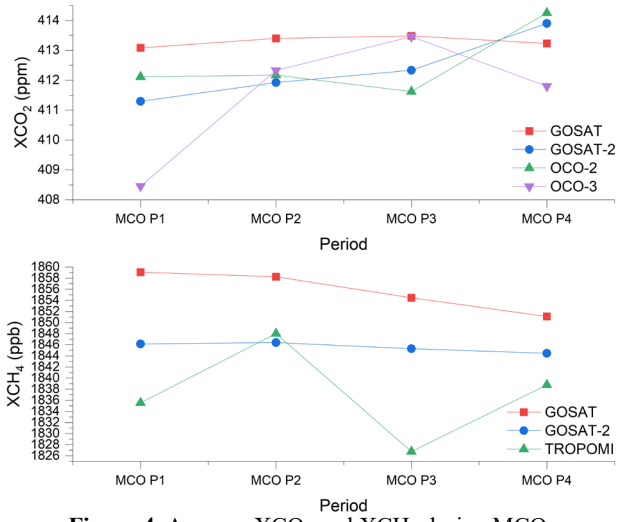

Figure 4. Average XCO_2 and XCH_4 during MCO.

Data		MCO		
		P1 to P2 (%)	P2 to P3 (%)	P3 to P4 (%)
XCO_2	GOSAT	+0.076	+0.020	-0.061
	GOSAT-2	+0.153	+0.100	+0.380
	OCO-2	+0.014	-0.133	+0.638
	OCO-3	+0.948	+0.275	-0.402
XCH_4	GOSAT	-0.044	-0.203	-0.182
	GOSAT-2	+0.014	-0.059	-0.045
	TROPOMI	+0.679	-1.15	+0.657

Table 2. Differences of average XCO_2 and XCH_4 during MCO phases.

It is noticeable that the XCO_2 and XCH_4 increases less than 0.95% while the largest decrease is approximately 1.15% during the phases of MCO.

3.2 Trends of XCO_2 and XCH_4 in industrial areas of States in Peninsular Malaysia during MCO (2020)

The average XCO_2 and XCH_4 from different satellite data for States in Peninsular Malaysia is observed in Figure 5.

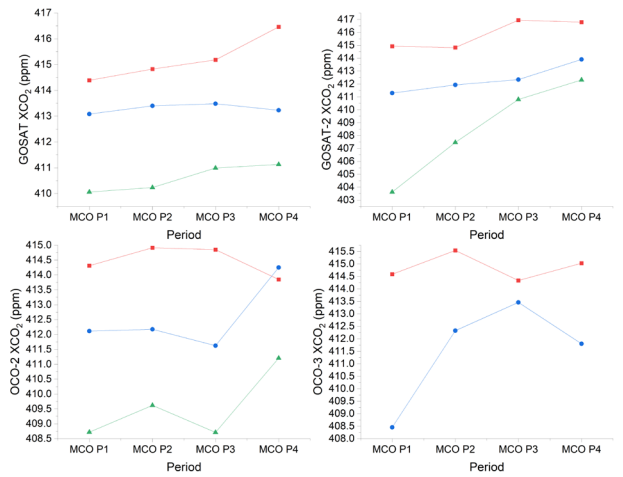

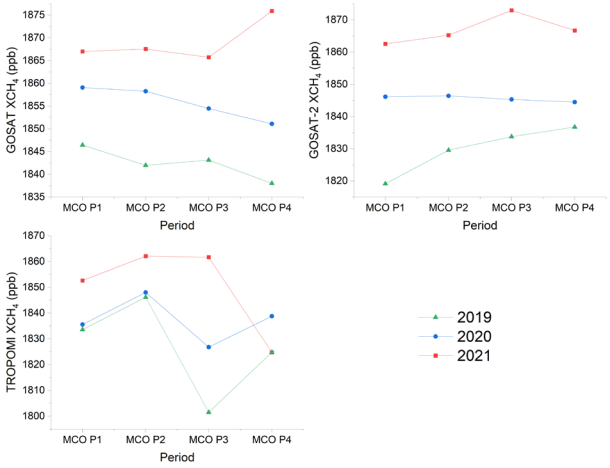

Figure 5. Average XCO_2 and XCH_4 in industrial areas of States during MCO.

The results revealed that the trend of the XCO_2 and XCH_4 show a similar trend for most of the States for almost all satellite data except for the GOSAT-2 XCO_2 and XCH_4 data which show a more distinct trends among States compared to other data. Among all States, the highest increase observed is approximately 1.4% and 1.25%, while the greatest decrease is about 0.75% and 1.6% for XCO_2 and XCH_4, respectively.

3.3 Discussion

From the results, it is observed that the XCO_2 and XCH_4 in industrial areas in Malaysia is increasing from year to year, by comparing the same periods among the years. Both XCO_2 and XCH_4 still show an increasing trend during the MCO although industrial activities are restricted. The study by Yusup et al. (2020) confirmed that MCO has limited impact on CO_2 concentration where the CO_2 concentration recorded at the Muka Head Station for March, April, and May 2020 is about 408.9, 424.2, and 428.6 ppm, respectively. MCO not affected the XCO_2 and XCH_4 much as a sudden decline in anthropogenic emission may not cause extensive declination in the overall concentration because CO_2 can reside in the atmosphere for 200 years while CH_4 has an atmospheric lifetime of approximately 12 years (Safaai et al., 2011).

Monitoring and mapping CO_2 and CH_4 in industrial areas with satellite data in Malaysia is challenging due to the geographic location of the country. As Malaysia is located in the tropics, the existence of optically dense clouds and aerosols limits the sampling density and data retrieval. Moreover, the design of the instrument hampered the mapping of the gases. Sparse sampling of GOSAT, GOSAT-2, OCO-2, and OCO-3, and large gap between neighbouring soundings make it difficult to cover the entire industrial areas. For instance, although having a high precision, only a small fraction is inspected by OCO-2 globally per day as it was aimed for sampling and not for mapping (Eldering et al., 2017). Therefore, the combination and use of multiple satellites data provides a better spatial coverage for continuous monitoring and mapping of the gases.

It is recommended that meteorological parameters such as wind speed and direction to be included in future work to study the wind effects on surrounding of the industrial areas and also determine the emissions sources. Industries with high emissions can be identified and actions can be taken to reduce the gases emitted into the atmosphere. On the other hand, IDW, a deterministic spatial interpolation method is employed due to its simplicity and fast calculation speed. Kriging is a more complex geostatistical spatial interpolation method and it can be applied in future work as the error map generated can be exploited for assessing the prediction accuracy of the interpolation map.

4. CONCLUSION

The XCO_2 and XCH_4 in industrial areas in Peninsular Malaysia during MCO are mapped successfully with satellites data from GOSAT, GOSAT-2, OCO-2, OCO-3, and TROPOMI. By comparing data during MCO period for the year 2019 to 2021, both XCO_2 and XCH_4 indicated an increasing trend from year to year and MCO has little influence on it. This work demonstrated that satellites data can be employed for continuous monitoring and mapping of CO_2 and CH_4 for large areas.

ACKNOWLEDGEMENTS

We would like to thank Malaysia Research University Network grant (R.J130000.7809.4L881 and R.J130000.7809.4L882), Ministry of Higher Education, Malaysia and UTM High Impact Research grant (Q.J130000.2409.08G97), Universiti Teknologi Malaysia for providing the funds and facilities for carrying out the research.

REFERENCES

Ash'aari, Z. H., Aris, A. Z., Ezani, E., Kamal, N. I. A., Jaafar, N., Jahaya, J. N., Manan, S. A., and Saifuddin, M. F. U., 2020: Spatiotemporal Variations and Contributing Factors of Air Pollutant Concentrations in Malaysia during Movement Control Order due to Pandemic COVID-19. *Aerosol and Air Quality Research* 20, 2047-2061.

Babulal, V., 2020: Air and water quality improve during MCO. https://www.nst.com.my/news/nation/2020/04/585488/air-and-water-quality-improve-during-mco, last access: 24 July.

Chevallier, F., Maksyutov, S., Bousquet, P., Bréon, F.-M., Saito, R., Yoshida, Y., and Yokota, T., 2009: On the accuracy of the CO_2 surface fluxes to be estimated from the GOSAT observations. *Geophysical Research Letters* 36, 5 pp.

Crisp, D., Pollock, H. R., Rosenberg, R., Chapsky, L., Lee, R. A. M., Oyafuso, F. A., Frankenberg, C., O'Dell, C. W., Bruegge, C. J., Doran, G. B., Eldering, A., Fisher, B. M., Fu, D., Gunson, M. R., Mandrake, L., Osterman, G. B., Schwandner, F. M., Sun, K., Taylor, T. E., Wennberg, P. O., and Wunch, D., 2017: The on-orbit performance of the Orbiting Carbon Observatory-2 (OCO-2) instrument and its radiometrically calibrated products. *Atmospheric Measurement Techniques* 10, 59-81.

Crowell, S., Baker, D., Schuh, A., Basu, S., Jacobson, A. R., Chevallier, F., Liu, J., Deng, F., Feng, L., McKain, K., Chatterjee, A., Miller, J. B., Stephens, B. B., Eldering, A., Crisp, D., Schimel, D., Nassar, R., O'Dell, C. W., Oda, T., Sweeney, C., Palmer, P. I., and Jones, D. B. A., 2019: The 2015-2016 carbon cycle as seen from OCO-2 and the global in situ network. *Atmospheric Chemistry and Physics* 19, 9797-9831.

DOE, 2021: Environmental Quality Report 2020, Department of Environment, Petaling Jaya, 178 pp.

Ducharme, J., 2020: World Health Organization Declars COVID-19 a 'Pandemic.' Here's What That Means. https://time.com/5791661/who-coronavirus-pandemic-declaration/, last access: 19 July.

Eldering, A., Wennberg, P. O., Crisp, D., Schimel, D. S., Gunson, M. R., Chatterjee, A., Liu, J., Schwandner, F. M., Sun, Y., O'Dell, C. W., Frankenberg, C., Taylor, T., Fisher, B., Osterman, G. B., Wunch, D., Hakkarainen, J., Tamminen, J., and Weir, B., 2017: The Orbiting Carbon Observatory-2 early science investigations of regional carbon dioxide fluxes. *Science* 358, 9 pp.

Hakkarainen, J., Ialongo, I., and Tamminen, J., 2016: Direct space-based observations of anthropogenic CO_2 emission areas from OCO-2. *Geophysical Research Letters* 43, 11400-11406.

Heymann, J., Reuter, M., Buchwitz, M., Schneising, O., Bovensmann, H., Burrows, J. P., Massart, S., Kaiser, J. W., and Crisp, D., 2017: CO_2 emission of Indonesian fires in 2015 estimated from satellite-derived atmospheric CO_2 concentrations. *Geophysical Research Letters* 44, 1537-1544.

Heymann, J., Reuter, M., Hilker, M., Buchwitz, M., Schneising, O., Bovensmann, H., Burrows, J. P., Kuze, A., Suto, H., Deutscher, N. M., Dubey, M. K., Griffith, D. W. T., Hase, F., Kawakami, S., Kivi, R., Morino, I., Petri, C., Roehl, C., Schneider, M., Sherlock, V., Sussmann, R., Velazco, V. A., Warneke, T., and Wunch, D., 2015: Consistent satellite XCO_2 retrievals from SCIAMACHY and GOSAT using the BESD algorithm. *Atmospheric Measurement Techniques* 8, 2961-2980.

Kaplan, G. and Avdan, Z. Y., 2020: Space-borne air pollution observation from Sentinel-5P TROPOMI: Relationship between pollutants, geographical and demographic data. *International Journal of Engineering and Geosciences* 5, 130-137.

Loheswar, R., 2020: Health Ministry confirms three cases on coronavirus infection in Malaysia. https://www.malaymail.com/news/malaysia/2020/01/25/health-ministry-confirms-three-cases-of-coronavirus-infection-in-malaysia/1831344, last access: 19 July.

Ma, J., 2020: Coronavirus: China's first confirmed Covid-19 case traced back to November 17. https://malaysia.news.yahoo.com/coronavirus-china-first-confirmed-covid-152553818.html, last access: 19 July.

MIDA, 2020: Chapter 9 Infrastructure Support, Malaysian Investment Development Authority, 82-90.

Nadzir, M. S. M., Ooi, M. C. G., Alhasa, K. M., Bakar, M. A. A., Mohtar, A. A. A., Nor, M. F. F. M., Latif, M. T., Hamid, H. H. A., Ali, S. H. M., Ariff, N. M., Anuar, J., Ahamad, F., Azhari, A., Hanif, N. M., Subhi, M. A., Othman, M., and Nor, M. Z. M., 2020: The Impact of Movement Control Order (MCO) during Pandemic COVID-19 on Local Air Quality in an Urban Area of Klang Valley, Malaysia. *Aerosol and Air Quality Research* 20, 1237-1248.

Parker, R. J., Boesch, H., Wooster, M. J., Moore, D. P., Webb, A. J., Gaveau, D., and Murdiyarso, D., 2016: Atmospheric CH_4 and CO_2 enhancements and biomass burning emission ratios derived from satellite observations of the 2015 Indonesian fire plumes. *Atmospheric Chemistry and Physics* 16, 10111-10131.

Safaai, N. S. M., Noor, Z. Z., Hashim, H., Ujang, Z., and Talib, J., 2011: Projection of CO_2 Emissions in Malaysia. *Environmental Progress & Sustainable Energy* 30, 658-665.

Sha, M. K., Langerock, B., Blavier, J.-F. L., Blumenstock, T., Borsdorff, T., Buschmann, M., Dehn, A., Mazière, M. D., Deutscher, N. M., Feist, D. G., García, O. E., Griffith, D. W. T., Grutter, M., Hannigan, J. W., Hase, F., Heikkinen, P., Hermans, C., Iraci, L. T., Jeseck, P., Jones, N., Kivi, R., Kumps, N., Landgraf, J., Lorente, A., Mahieu, E., Makarova, M. V., Mellqvist, J., Metzger, J.-M., Morino, I., Nagahama, T., Notholt, J., Ohyama, H., Ortega, I., Palm, M., Petri, C., Pollard, D. F., Rettinger, M., Robinson, J., Roche, S., Roehl, C. M., Röhling, A. N., Rousogenous, C., Schneider, M., Shiomi, K., Smale, D., Stremme, W., Strong, K., Sussmann, R., Té, Y., Uchino, O., Velazco, V. A., Vrekoussis, M., Wang, P., Warneke, T., Wizenberg, T., Wunch, D., Yamanouchi, S., Yang, Y., and Zhou, M., 2021: Validation of Methane and Carbon Monoxide from Sentinel-5 Precursor using TCCON and NDACC-IRWG stations. *Atmospheric Measurement Techniques Discussions*, 84 pp.

Shim, C., Han, J., Henze, D. K., and Yoon, T., 2019: Identifying local anthropogenic CO_2 emissions with satellite retrievals: a case study in South Korea. *International Journal of Remote Sensing* 40, 1011-1029.

Srivastava, P., Bennett, M. W., Bedrosian, G., Rosenberg, R., Solish, B., and Basilio, R. R.: Establishing Launch Readiness of NASA ISS Instrument OCO-3, 2020 IEEE International Geoscience and Remote Sensing Symposium (IGARSS 2020), Hawaii, USA, 26 September - 2 October, 6101-6104,

Suto, H., Kataoka, F., Kikuchi, N., Knuteson, R. O., Butz, A., Haun, M., Buijs, H., Shiomi, K., Imai, H., and Kuze, A., 2021: Thermal and near-infrared sensor for carbon observation Fourier transform spectrometer-2 (TANSO-FTS-2) on the Greenhouse gases Observing SATellite-2 (GOSAT-2) during its first year in orbit. *Atmospheric Measurement Techniques* 14, 2013-2039.

Taylor, T. E., Eldering, A., Merrelli, A., Kiel, M., Somkuti, P., Cheng, C., Rosenberg, R., Fisher, B., Crisp, D., Basilio, R., Bennett, M., Cervantes, D., Chang, A., Dang, L., Frankenberg, C., Haemmerle, V. R., Keller, G. R., Kurosu, T., Laughner, J. L., Lee, R., Marchetti, Y., Nelson, R. R., O'Dell, C. W., Osterman, G., Pavlick, R., Roehl, C., Schneider, R., Spiers, G., To, C., Wells, C., Wennberg, P. O., Yelamanchili, A., and Yu, S., 2020: OCO-3 early mission operations and initial (vEarly) XCO_2 and SIF retrievals. *Remote Sensing of Environment* 251, 27 pp.

WHO, 2022: Coronavirus disease (COVID-19). https://www.who.int/health-topics/coronavirus#tab=tab_1, last access: 24 July.

Wu, L., Brugh, J. a. d., Meijer, Y., Sierk, B., Hasekamp, O., Butz, A., and Landgraf, J., 2020: XCO_2 observations using satellite measurements with moderate spectral resolution: investigation using GOSAT and OCO-2 measurements. *Atmospheric Measurement Techniques* 13, 713-729.

Yang, Y., Zhou, M., Langerock, B., Sha, M. K., Hermans, C., Wang, T., Ji, D., Vigouroux, C., Kumps, N., Wang, G., Mazière, M. D., and Wang, P., 2020: New ground-based Fourier-transform near-infrared solar absorption measurements of XCO_2, XCH_4 and XCO at Xianghe, China. *Earth System Science Data* 12, 1679-1696.

Ye, X., Lauvaux, T., Kort, E. A., Oda, T., Feng, S., Lin, J. C., Yang, E. G., and Wu, D., 2020: Constraining Fossil Fuel CO_2 Emissions From Urban Area Using OCO-2 Observations of Total Column CO_2. *Journal of Geophysical Research: Atmospheres* 125, 29 pp.

Yusup, Y., Ramli, N. K., Kayode, J. S., Yin, C. S., Hisham, S., Isa, H. M., and Ahmad, M. I., 2020: Atmospheric Carbon Dioxide and Electricity Production Due to Lockdown. *Sustainability* 12, 12 pp.